Jestr

Journal of Engineering Science and Technology Review 6 (5) (2013) 149 -164

JOURNAL OF
Engineering Science and Technology Review

www.jestr.org

Research Article

Substorm – associated Dual System of Field-Aligned Currents interpreting Major Bipolar Magnetic Field Signatures in the Earth's Magnetotail

D. V. Sarafopoulos

Department of Electrical and Computer Engineering, Democritus University of Thrace, Xanthi, Greece

Received 1 November 2013; Accepted 28 December 2013

Abstract

We investigate in detail seven "magnetic flux rope (MFR) like structures" successively occurring in a storm-time interval of 9 min using the four-point satellite measurements of the Cluster tetrahedron in the Earth's magnetotail. Our major finding is that in all these structures, **the main magnetic field signatures could be well reproduced by a dual filamentary system of field-aligned currents (FACs) flowing earthward**; one branch in northern and the other in southern plasma sheet. And under this current topology the B_y deviations might well result as an effect of Ampere's law. In three (out of the seven MFR-like structures) opposite polarities for the B_y excursions are simultaneously observed by satellites placed (in plasma sheet) symmetrically with respect to the neutral sheet. In one case, we diagnose a filamentary FAC limited in a channel with ΔY thickness about 1000 km; while, at the same time, the whole channel propagates dawnward. We also scrutinize in detail all the remaining characteristic B_y and B_z signatures within the same interval; the conclusion is that persistently earthward flowing FACs suffice to derive all these additional Cluster signatures. Therefore, a supply mechanism (for these FACs) seems to be always at work; and it is imperative to search for a candidate mechanism. To this direction we especially discuss the recently introduced by Sarafopoulos [1] "twin-double layer model" having the capability of producing oppositely directed and highly jetting ions along the central plasma sheet (CPS) magnetotail. Each jet, flowing outward from its source with progressively increasing speed, accumulates positive charges at its propagation front. And in this way it increases the local cross-tail current and eventually builds up a strong barrier of positive B_z magnetic field being the key element for the typical MFR-like structure (at a site where otherwise the B_z is exceptionally weak). Several B_y deviations are clearly not related to the persistently positive B_z direction of the interplanetary magnetic field (IMF). The MFR-like structures are identified on the basis of their morphological magnetic field signatures, that is (a) a strong B_y deviation, (b) a bipolar B_z perturbation and (c) an increase of the total magnetic field amplitude. The "pseudo-MFR" shows almost the same observational features as described above but is actually produced by a travelling waveform of a filamentary FAC.

Keywords: Field-aligned currents, plasma sheet, magnetic reconnection, double layers, magnetic flux rope, , solar wind-magnetosphere interaction.

1. Introduction

The purpose of this work is not to demonstrate that real MFRs are non-existing. The latter is particularly apparent in a recent work of Sarafopoulos [2], where often the core of typical MFRs is associated with an "ion vortex", an ion cyclic current within the plasma sheet. In parallel, the main effort in this work is obviously not to show that "pseudo-MFRs" really exist, but to establish that two branches of parallel FACs symmetrically placed with respect to the neutral sheet (in the Earth's magnetotail) are developed, at times, using an indicative case study with four satellites. Signatures very similar to those observed in real ropes are probably produced by the wavy modulated filamentary FACs; these structures are so-called pseudo-MFRs.

The observational part and its associated interpretation, as set forth in this work, are coupled through a newly introduced model capable to explain the field-aligned currents (FACs) which are considered as necessary when trying to reproduce the major magnetic field signatures observed throughout an indicative interval of CLUSTER in plasma sheet. In particular, the main components are as follows: **firstly,** the basic concept introduced by Sarafopoulos [3] is more thoroughly and systematically scrutinized. He investigated two notable events using the THEMIS satellites, for the one case, and the Cluster mission, for the other, and concluded that the magnetic field signatures associated with his "two magnetic flux rope (MFR) like structures" can be readily reproduced by filamentary FACs flowing earthward and being wavy modulated over the meridian XZ plane. He detected an (almost simultaneously) MFR-like structure with a **positive B_y excursion for THEMIS-C** and a **negative for THEMIS-B**; an apparent inconsistency for the same entity supposed to be the MFR's core. For the first time strong evidence was provided that effects of Ampere's law may have been previously interpreted as MFRs embedded in tailward plasma flows. He also applied the same explanation

* E-mail address: sarafo@ee.duth.gr

ISSN: 1791-2377

upon "a rare Cluster phenomenon" that was previously cited in literature and categorized as "an irregular, complicated MFR structure" [4]. In this work, we undertake an effort to demonstrate that **tens of B_y and B_z signatures** (observed in succession during a very indicative interval of 9 min, and irrespectively of being associated or not with MFR-like structures), can be (qualitatively) well reproduced by two branches of filamentary FACs: one branch in northern and the other in southern plasma sheet. Amid very high geomagnetic activity, we did not probably detect any authentic MFR entity that would be associated with the dramatic magnetic field reconfigurations. Thus, each B_y deviation really seem to be the effect of Ampere's law (and not the rope's core itself). **Secondly,** in our interpretation scheme, we adopt a mechanism that potentially produces the required dual system of FACs; the latter is based on the recently published work by Sarafopoulos [1] introducing "a twin-double layer (DL) structure" as the ultimate source having the capability of launching oppositely directed high velocity ion jets along the magnetotail. The currently proposed interpretation scheme is exhibited immediately below in subsection 2, although the completely elaborated mechanism concerning specifically "the twin-DL source" can be found in the above cited work. We establish all our results using the Cluster mission experiments as a powerful tool delivering impressive four-point measurements. During the studied interval there are intense plasma flows in central plasma sheet (CPS), while five flapping cycles take place in magnetotail. We study successive and strong B_y excursions for which the discrimination between temporal and spatial effects is beyond any uncertainty. Thus, we clearly infer that the occurrence of "pseudo-MFRs" seems to be rather a common event; they are not extraordinary epiphenomena. Throughout the text, at times, we use the word "core" or the expression "B_y deviation or excursion" indiscriminately; it is inevitable although these terms better match to an MFR or a filamentary current, respectively.

Schindler [5] and Hones [6] developed theories regarding the macroscopic effects of two dimensional (2-D) reconnection upon the magnetic topology of the Earth's magnetotail; later, the identification of the three dimensional (3-D) MFR structures radically changed the whole scenery. Sibeck et al., [7] recognized structures in the distant magnetotail having the characteristics of the flux ropes studied by Russell and Elphic [8] over the dayside magnetopause: a strong axial magnetic field is surrounded by a weaker circumferential magnetic field; the observed signatures often show a peaked B_y magnetic perturbation when the B_z reverses its direction.

Intensive investigation was then undertaken using the more comprehensive instrumentation carried by Geotail. It is assumed that the 2-D magnetic loop topologies considered by Schindler and Hones are not achievable in 3-D because perfect alignment of the oppositely directed magnetic field lines would be required: The forces exerted at the magnetopause by reconnection act to shear the two lobes and impress a small B_y throughout the magnetosphere [9]. Hughes and Sibeck [10], Birn et al. [11], and Moldwin and Hughes [12] demonstrated that this small B_y in the plasma sheet leads naturally to the generation of magnetic ''flux ropes'' instead of ''loops'', when reconnection takes place. Therefore, in the Earth's magnetotail, the B_y is generally attributed to IMF driving and smaller-scale internal dynamics. Petrukovich [13, 14] constructed a new detailed statistical model of plasma sheet B_y and inferred that the IMF-B_y penetration for the whole data set was 0.35, in general agreement with previous studies (references there in). Moreover, they introduced additional factors affecting the B_y; we shall discus their works later on.

Although the magnetic fields within ropes are often irregular and complex (e.g., [4]), they have a clear tendency toward helical magnetic field topologies [15-19]. The electric current can be either parallel or antiparallel to the sense of the magnetic field lines in the flux rope. Recent Cluster investigations have expanded our knowledge on MFRs (e.g., [20-23]). In general, often MFRs have been suggested to be part of a "multiple-reconnection X-line" scenario [24]. In this scenario, N+1 X-lines lead to the formation of N flux ropes in between them. One of these X-lines is then believed to outpace the others, and will be the first to reconnect open field lines in the lobes. This X-line will then become the major, active X-line in the sense of the NENL substorm model [25-28], and it will divide up the regions of earthward and tailward flows in the magnetotail. However, we have to stress that the MFR generation mechanism rather remains a controversial issue (e.g., [4, 23]). Sarafopoulos [2] proposed a specific mechanism that may determine the sign of the core for an MFR; frequently the tail bends upward (northward) or downward (southward) and the particular type of motion dictates the rope's sign.

The interval under research has been approached in the past by many researchers (e.g., [29-32]). However, for the first time, we essentially focus on the MFR-like structures and the associated FACs; a radically different point of view.

The combined Cluster datasets, used in this work, finally prove that all the strong B_y deviations are probably produced by filamentary FACs. In parallel, it is suggested that the ultimate cause for the FACs is the ion jets produced in CPS. The ion jet mechanism is supposed to be "the twin-DL source" which generates large scale charge separations affecting the cross-tail current and feeding the FACs. The tailward ion jet, ahead of its propagation front, probably produces the strong B_z component of the magnetic field observed in CPS and related to the supposed MFR.

Additionally, more of the presently studied "MFRs" show the opposite B_y polarity than that which would be potentially dictated from the sign of B_y of the interplanetary magnetic field (IMF).

2. The Suggested Interpretation Model

Before we present the observational part of this work, we introduce an interpretation model that best fits our datasets. Apparently it does not comply with main existing models: For instance, the reconnection model may be related to FACs flowing outward (i.e., Ew and Tw) from an X-line "ion diffusion region"; nevertheless, as we shall infer in this work, **always FACs flowing constantly earthward are needed**. Consequently, we look for a model to generate this type of currents. We essentially introduce a model based on the recently published work of Sarafopoulos [1], and point to **Fig. 1** a "unified picture" potentially able to derive all the observed major magnetic field signatures. The focal point in this picture, denoted by DL, is positioned somewhere within the near Earth (locally thinned) plasma sheet, where the ions essentially lose their adiabatic motion and eventually form the twin-double layer (DL) structure (as it is analytically elaborated in the above cited work) **producing two oppositely directed ion jets** along the magnetotail. In its explosive phase, the twin-DL source has the capacity to produce ion jets with very high velocities and energetic particle fluxes as well. In general, for each jet the velocity progressively increases and, as a result, two magnetic structures are built up in front of the leading edges of earthward (Ew) and tailward (Tw) flows. The temporal evolution of the source, tightly associated with the rapidly increasing ion velocity, leads to an ion accumulation close to both propagation fronts; **the faster ions catch up the slower ones**. This way the localized intense cross-tail currents generate two well-built structures characterized by positive B_z increases, Ew and Tw of the (DL) source, at the very CPS region. Within the Plasma Sheet the formation of two "B_z barriers" with dominant component the B_z is of crucial importance. The "B_z barrier" at the right-hand part of source forms the so-called "ion capsule" [33, 34, 3, 2], which is tightly coupled with the Tw ion jet. Finally, the "B_z barriers" move in the directions Ew and Tw, as it is dictated from the ion jets and the tailward DL motion; the magnetic flux piles up earthward of DL. Therefore, a satellite seems to cross these structures moving Tw for Ew jets and Ew for Tw jets: a situation visualized by the indicative satellite trajectories Tr-1 and Tr-2, respectively, in Fig. 1. Since the ion jets reflect the tail's internal dynamics, these two trajectories are the typical satellite paths coupled with $-B_z/+B_z$ bipolar signatures for Ew jets and $+B_z/-B_z$ signatures for Tw jets. At the same time, the locally intense ion charges, which are ejected from the source, have to be neutralized by FACs. These currents always flow Ew and adjacent to the lobes (blue arrows). Consequently, whenever the B_z changes sign (trajectories Tr-1 and Tr-2), an additional peaked B_y deviation is caused by the FACs flowing along the flanks of "the ion capsules". Moreover**,** one may add tail's motions that dramatically change the eventually observed magnetic field signatures, although the intra-plasma sheet physical mechanisms presumably remain the same. For instance, if the vertical (upward or downward) tail's motion prevails, the satellite trajectories would be similar to the Tr-3 and Tr-4 cases sketched in Fig. 1. Each trajectory now must be associated with two similar B_y bipolar signatures: a $+B_y/-B_y$ bipolar signature during the entry into the plasma sheet and an additional $+B_y/-B_y$ signature during the exit out of it**. In between the two parallel FACs we should detect a $-B_y/+B_y$ signature**. In a different mode of tail's motion, we would detect exclusively bipolar signatures of B_z. For instance, if a tilted (relatively to the Y-axis, see **Fig. 2**) tail moves duskward, which is equivalent with a satellite (S/C) moving dawnward (over the YZ cross-sectional plane) and completely crossing the tail plus the two accompanying branches of FACs, then one would detect the same $+B_z/-B_z$ signature at the entry into and at the exit out of the plasma sheet.

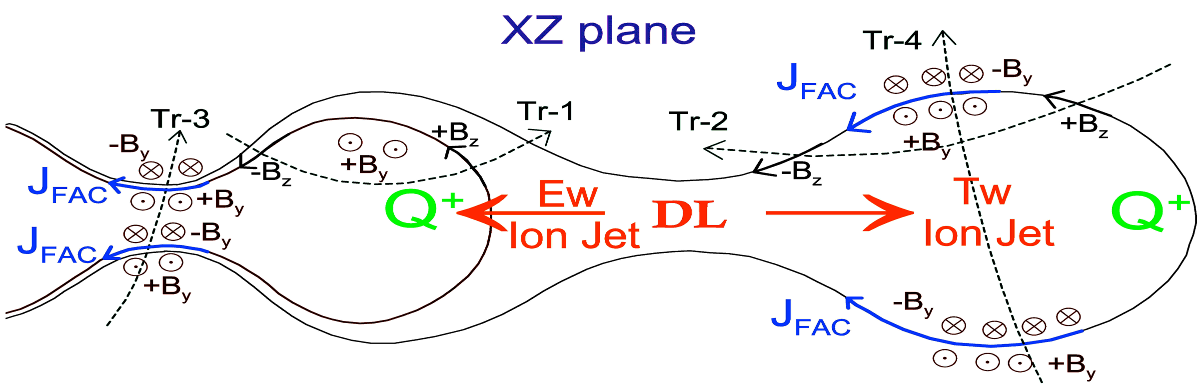

Fig. 1. The twin-double layer source located at the "DL" site produces two oppositely directed ion jets in a locally thinned plasma sheet. Each ion jet builds up an intense Bz barrier in CPS (around the area marked by Q+) and, at the same time, feeds the appropriate FACs. A variety of satellite trajectories result from the tail's flapping (cases Tr-3 and Tr-4) or the internal tail's dynamics (cases Tr-1 and Tr-2) or "a mixed mode" combining both of the just mentioned motions. The magnetic field signatures are dictated by the FACs flowing earthward along the magnetic field lines and the specific trajectory path in case.

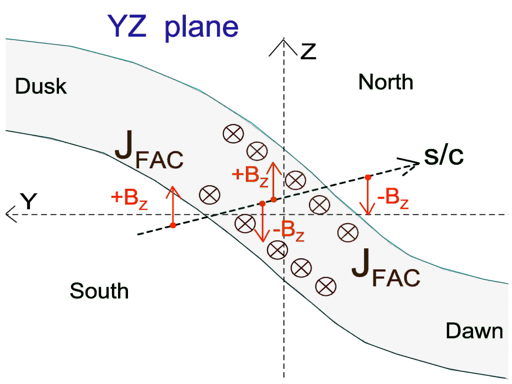

Fig. 2. The tilted (relatively to the Y-axis) tail moves duskward carrying the two accompanying branches of FACs. However, in this schematic a satellite (S/C) is shown moving dawnward (over the cross-sectional YZ plane), crossing the whole tail and detecting the same $+B_z/-B_z$ signature at the entry into and at the exit out of the plasma sheet.

In summary**:** The B_z and B_y magnetic field signatures are depended on, in a large degree, the tail's motions, and additionally, they are directly or indirectly associated with the plasma sheet ion jets reflecting the tail's internal dynamics, at substorm-times. The finally recorded signatures may concern exclusively the B_z or the B_y component or both of them. If the B_z and B_y traces show "a mixed mode", with characteristic deviations in both components at the same time, then we infer that an MFR-like structure is formed. From 09:41:20 to 09:50 UT (being the studied interval with about 9-min duration) the magnetotail displays a quasi-periodic flapping; five variation cycles are recorded by Cluster as ten successive crossings of the (entire, at times) plasma sheet. Consequently, such a repetitive mode of crossings associated with a variety of bipolar and/or monopolar B_z and B_y signatures provide the unique opportunity to reveal the fundamental role of (existing) FACs in the magnetotail's dynamics.

3. Observations

3.1. Satellite Positions, Experiments, Storm-Time Period

First we investigate the MFR-like structures identified within the interval 09:41:20-09:50 UT of October 1 (day 274), 2001, based on their magnetic field signatures. It is a storm-time period: The D_{st} index is -148 nT and the AE index is greater than 500 nT. Later on, we shall show that the (storm-time) B_z component of the IMF has an intense and persistently negative value leading to an enhanced solar wind-magnetosphere electromagnetic coupling. During this interval, we mainly analyze three events; two double- and one triple-MFR-like structures, and totally in all seven episodes. The occurrence time for each event is marked with a vertical dashed-thick-red line in Fig. 3. The first two events are characterized by earthward plasma flows (top panel, look at ~09:42:40 and 09:44:10 UT) and the third event is associated with tailward flow (at ~09:47:30 UT); the MFRs seem to be embedded in earthward or tailward flows. Throughout our research the four Cluster satellite datasets and the satellite trajectories are indicated by the same color code: C1 with black, C2 with red, C3 with green and C4 with blue. In **Fig. 3**, the three components of plasma velocity (top two panels) are shown along with the proton plasma density (third panel, in cm^{-3}) recorded by C4, and the B_x components of the magnetic field (bottom panel, in nT) for the C1 and C4 satellites. The green line (in bottom panel) is the sin function that matches up with the magnetotail flapping motion demonstrating a periodicity of ~100 s. This period is apparently much larger than the duration of one MFR-like structure typically lasting less than 15 s. Below we perform detailed analysis for each case study and suggest an interpretation. Finally, we infer that a dual filamentary current system suffices to produce all the observed magnetic field signatures associated with the MFR-like structures. Then, four more subintervals, marked with vertical-thin-reddish lines in Fig. 3, are briefly scrutinized demonstrating that similar FACs are always at work in this period. During the interval under research, the tetrahedron of Cluster satellites is placed in the Earth's magnetotail, at $(X, Y, Z)_{GSE}$=(-16.3, 6.4, 5.08) R_E. This tetrahedron projected over the XY, XZ and YZ planes (blue-violet quadrangles) in the GSE coordinate system, at 09:47 UT, is shown in **Fig. 4**. At the same time, the Geotail satellite was located upstream of the bow shock, at $(X, Y, Z)_{GSE}$=(17, -17.6, 0.56) R_E. The solar wind velocity is V_x= -480 Km s^{-1} and the estimated propagation time Δt (from Geotail to Cluster) is ~6 min. More accurate value of Δt is not an issue of crucial importance, **since the B_y of the IMF persistently remains positive**, and we are interested in for the interrelationship of polarities between IMF-B_y and MFR-B_y; the latter is definitely answered in the discussion section.

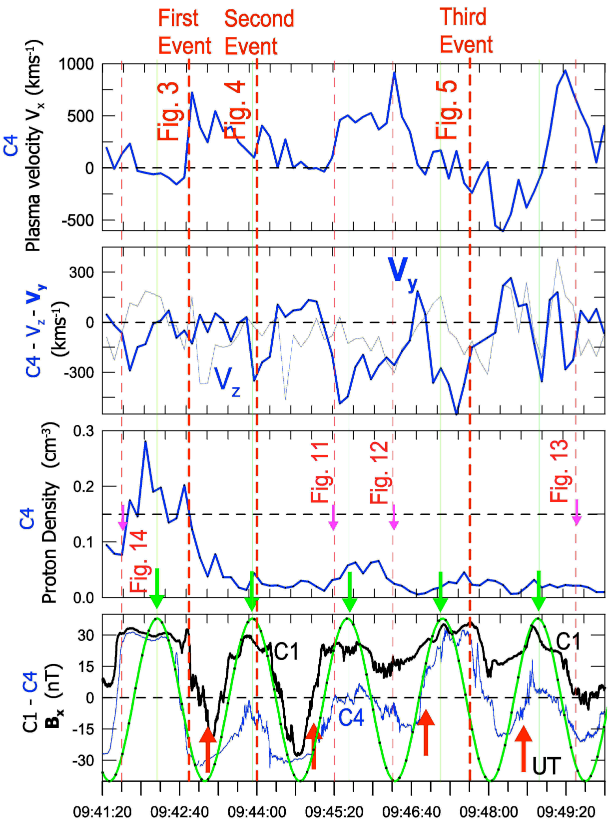

Fig. 3. Three components of proton plasma velocity and proton density, measured by the C4 satellite, along with the B_x components of the magnetic field recorded by C1 (thick-black line) and C4 (thin-blue line). The three studied main events (two with earthward flows plus one with tailward flow) are marked with vertical red-thick-dashed lines. The green-dotted line is a sine-wave function with T=100 s. The vertical-thin-dashed lines correspond to the additional four studied subintervals

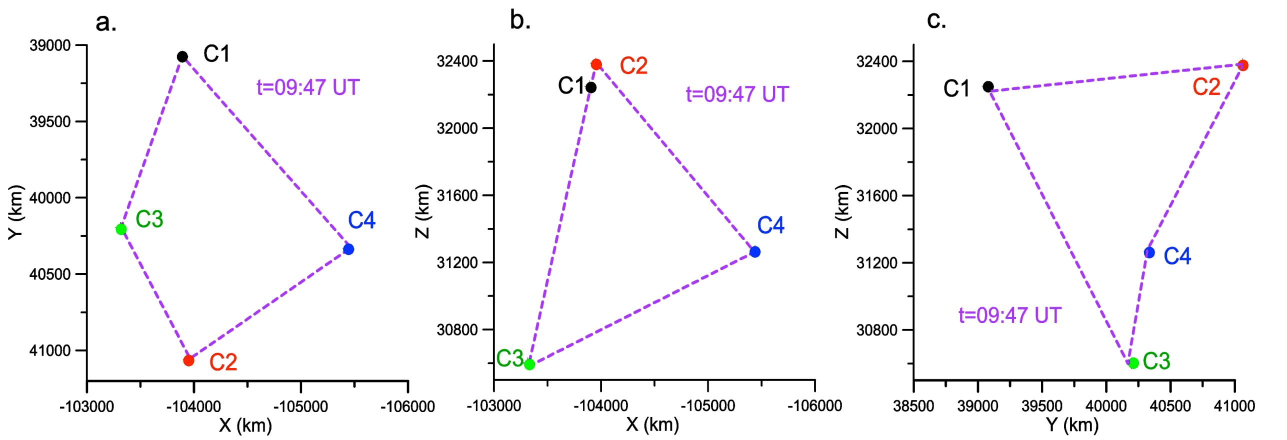

Fig. 4. Blue-violet quadrangles showing the Cluster tetrahedron projected over the planes XY, XZ and YZ (a-b-c panels, respectively) for the instant t=09:47 UT. The satellite positions are given in the GSE coordinate system.

The Cluster data, discussed in this work, were obtained by the Flux-Gate Magnetometer (FGM; [35]) from the four spacecraft, and by the Cluster Ion Spectrometry (CIS; [36]) experiment from Cluster 1, 3, and 4. All the Cluster magnetic field measurements are shown (Figs 3-14) in the GSE coordinate system. As we shall be convinced later on, the B_y deviations (in this work) are characterized by very small durations; therefore, they are probably not "cores" aligned along the Y_{GSM}-axis and extended to many R_E, as it is the situation in typical-real ropes. In contrast, since the studied structures are most likely the effects of filamentary currents (mainly flowing along the X-axis), it results that there is not any particular obligation to use the GSM coordinate system.

Throughout the presentation, the term "MFR" is used as in the literature, in the mainstream research efforts. That is, an MFR is considered as "an outer layer" of magnetic field that forms the tubular-helical structure around "the inner layer" that constitutes its core. In practice, we initially identify an MFR by its morphological magnetic field signatures [37, 20], that is (a) the B_y-component strong excursion (from its local average value) forming ''the core'' of the supposed rope; (b) the B_z-component characterized by a bipolar feature at the time the B_y is peaked and corresponding to the helical magnetic field structure; and (c) the total magnetic field-B_{total} increase at the same time. Each MFR-like structure is accompanied by a tailward or earthward plasma flow. In the discussion section, we shall further elaborate our concept about their production mechanism.

3.2. First Event, a Double MFR-Like Structure

This event occurs with a rapid earthward (Ew) plasma flow having velocity $V_x \approx 500$ km s^{-1}. It lasts ~40 s, an interval which is essentially characterized by a transition from the north to south lobe; that is, we actually observe a northward magnetotail flapping which is representatively demonstrated by the C2 and C3 magnetic field datasets (**Fig. 5**, look especially at the B_x traces, second panel). Two distinct and successive MFR-like structures are clearly characterized by all the morphological MFR-associated features. For instance, C2 (red line) displays, at t_2 and t_3, (a) two major excursions of B_y (first a positive, then a negative one, third panel), (b) two bipolar south-then-north signatures (look at the fourth panel for the B_z trace and at the fifth panel for the theta-polar angle trace of magnetic field), and (c) two distinct increases of the total magnetic field (first panel). Similarly, C3 (green line with triangles) at t_1 and t_2 displays two major B_y excursions (first a positive and soon after a negative one, third panel).

The positive B_y deflection of ~20 nT (being potentially the core for the "first MFR") is initially seen by C3 and soon after by C2 at the moments t_1 and t_2, respectively. Subsequently, C3 at t_2 and C2 at t_3 (around 09:42:58 UT) show negative excursions with maximum $|\Delta B_y| \approx 20$ nT. The negative excursions may constitute "the core" for the so termed "second MFR-like structure". Again, let us pay attention to Fig. 5: **while C3 and C2 cross the whole plasma sheet, their B_y traces demonstrate similar patterns.** The B_y excursions are positive (for C2 and C3 alike) within the plasma sheet and adjacent to the north lobe; conversely they are negative within the plasma sheet and adjacent to the south lobes. The peaked values along the C2-B_y and C3-B_y traces occur within the plasma sheet and closer to the lobes. The dashed-red line (drawn in third panel) is the third order polynomial fitting for the C2-B_y trace. Consequently, the entry into the plasma sheet is associated with positive B_y deviation, whereas before the exit out of the south plasma sheet is related a negative B_y one. Most importantly, at t_2**, we simultaneously observe positive and negative** B_y deviations for C2 and C3, respectively! Obviously, as we argue below, these two deviations are not two distinct entities (related really to ropes extended along the Y-axis); the strong B_y excursions most likely originate from filamentary currents.

The well ordered and time-shifted excursions of B_y **are mainly due to spacecraft placement over the XZ plane** (Figs. 4b and c): C3 being located closest to the neutral sheet first entering into the plasma sheet and first crossing the neutral sheet. C4 follows and C2 was located further away from neutral sheet; the intersatellite distance between C3 and C2, along the Z-axis, is ΔZ=1780 km, about the thickness of the plasma sheet. Thus, since the tail is flapping upward, we first observe the positive C3-B_y excursion and soon after the C2-B_y. The C1 and C4 traces are not included in Fig. 3, since C4 does not carry any significant additional information and C1 is widely separated from all the other satellites in respect to the Y-axis.

Interpretation: Since this event occurs with rapid earthward plasma flow and a simultaneous northward flapping of the tail, Cluster in Fig. 1 (a) moves along the Tr-1 trajectory and (b) traverses the whole plasma sheet in a way similar to that indicated through the Tr-3 trajectory (although in the reverse direction actually). Combination of both "independent motions" can derive the final features observed in Fig. 5: (a) the bipolar +B_y/-B_y signature seen (symmetrically) around the neutral sheet by both C2 and C3, and (b) the bipolar -B_z/+B_z signature clearly seen only by C2 at times t_2 and t_3.

3.3. Second Event, a Triple MFR-Like Structure

Three successive MFR-like structures occur during the 100-s interval presented in **Fig. 6**. In particular, we observe three (intense and successive) negative B_y deflections captured by C2 at time instants t_1, t_2 and t_3 (third panel, thick-red line). Simultaneously, the total magnetic field is peaked (top panel) for every one excursion (marked with a vertical blue-dashed line). Additionally, all the three structures are also associated with B_z transitions from negative (or less positive) to more positive values with respect to the earthward observed plasma flow (Fig. 3). Consequently, all the morphological characteristics, for each of the three successive MFRs, are clearly satisfied.

The C1 and C4 satellites do not carry any significant information (in our analysis); consequently, their magnetic field measurements are not included in Fig. 6. During this interval, C1 stays close to the north lobe for a long time, while C4 shows a time-shifted B_y profile similar to that of C3; the latter is obviously due to the large ΔX separation distance between C3 and C4 being 2170 km. The profound dissimilarity between the plotted C2- and C3-B_y traces is due to their vertical-ΔZ separation distance being 680 km, as it becomes clear below.

The "first MFR-like structure" reveals that the peak C2-B_y value is about -15 nT; in contrast, C3 (green-dotted line) unexpectedly records at the same time a positive B_y excursion with maximum value ~10 nT. Similarly, for the "second MFR", **B_y deflections with opposite polarities are recorded by C2 and C3**. During the "third MFR", C3 does not detect any B_y variation since it passed into the lobe.

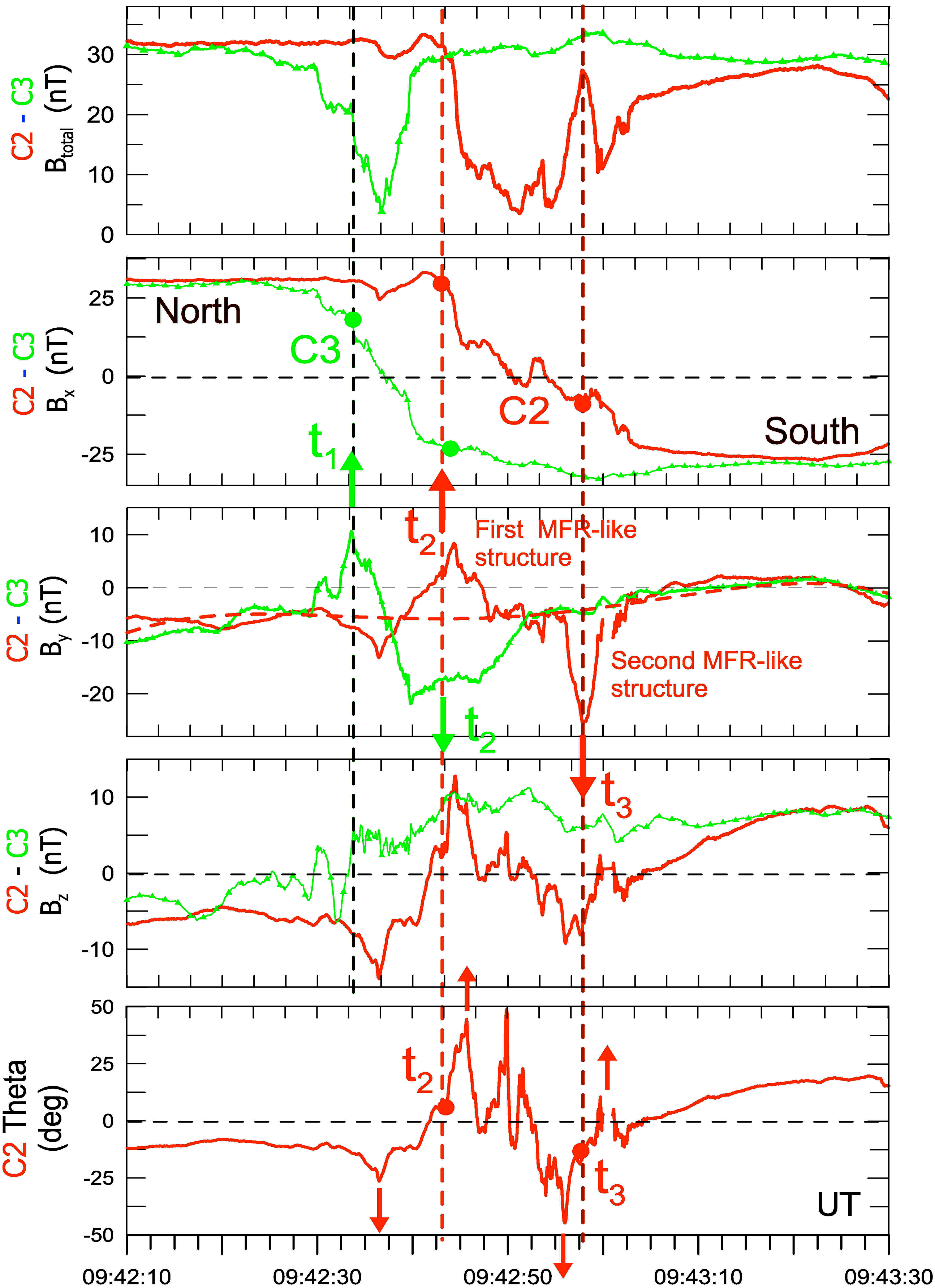

Fig. 5. Vector magnetic field measurements for the C2 and C3 satellites traversing the plasma sheet. Positive and negative C2-B_y excursions (at t_2 and t_3, third panel) corresponding to the "first and second MFR-like structures" are accompanied by two bipolar south-then-north signatures and B_{total} increases. At the bottom panel the theta-polar angle variations are shown for C2. Particularly at t_2, positive and negative B_y deflections are detected simultaneously by C2 and C3. All the Cluster magnetic field datasets are displayed in the GSE coordinate system.

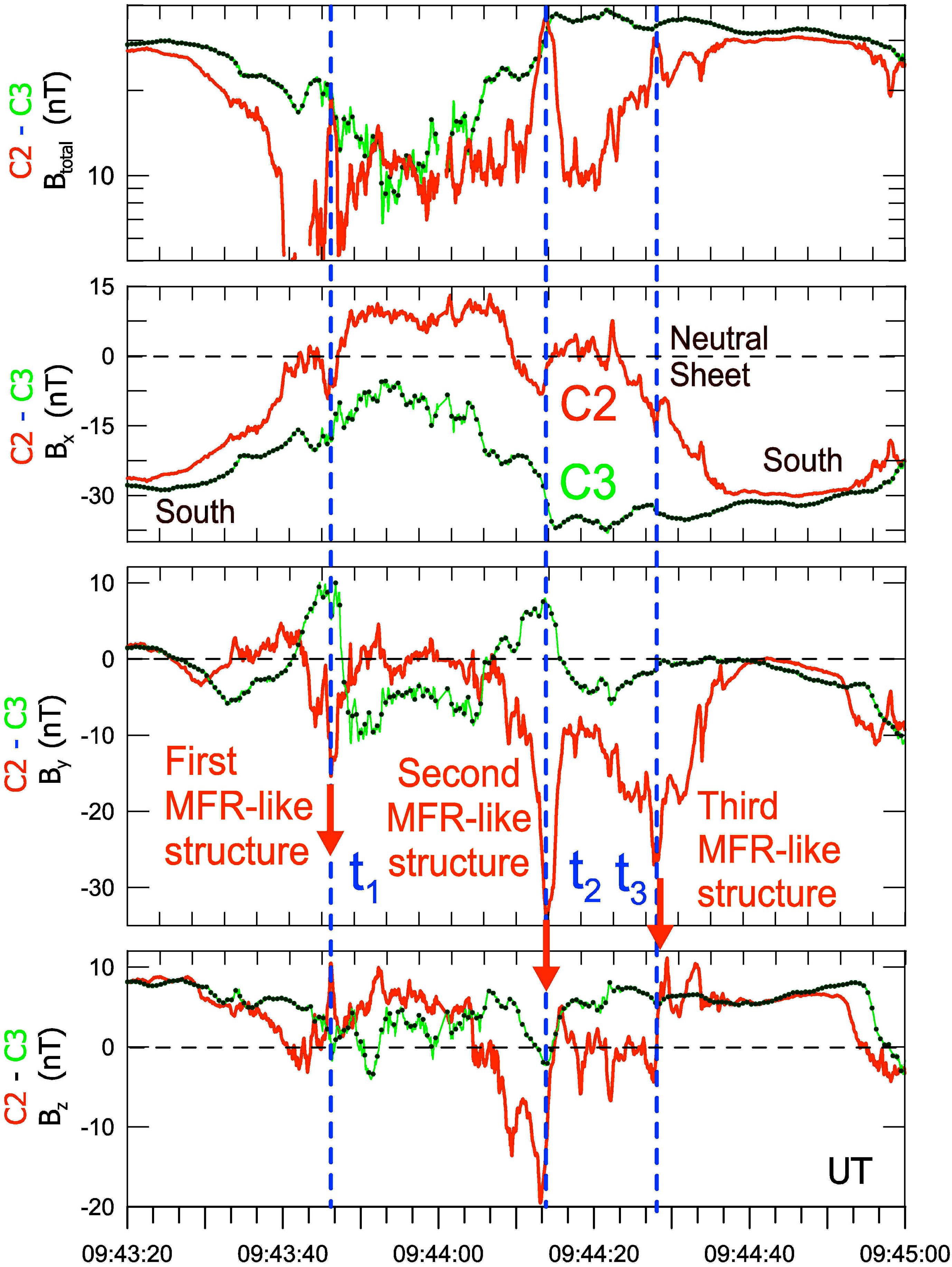

Fig. 6. Vector magnetic field datasets for C2 and C3. The three strong-negative B_y excursions of C2 (third panel), at the time instances t_1, t_2 and t_3, correspond to south-then-north signatures of B_z (fourth panel) and increases of the total magnetic field (first panel); three MFR-like structures are marked with vertical-dashed lines. We observe opposite polarities between C2-B_y and C3-B_y at t_1 and t_2.

In Fig. 6, C2 and C3 set off from south lobe, move toward the neutral sheet and finally return to their initial positions. The three MFR structures are related to theta angle transitions from -45^o to 30^o, -40^o to 22^o, and from -8^o to 28^o (not shown here). As we shall present immediately below, all the B_y magnetic field signatures can be readily interpreted as effects due to a filamentary current flowing earthward somewhere between the south lobe and the neutral sheet.

Interpretation: **Figure 7** is sketched, over the XZ plane, illustrating the manner in which the main magnetic field signatures are derived. As a matter of fact, only one current branch from the dual system of FACs (adopted in Fig. 1) suffices for the present situation. The satellite trajectories are shown with dashed-red and -green lines for C2 and C3, respectively, on the basis of diamagnetic depressions of B_x. The supposed (filamentary) FAC is depicted (in parallel to the neutral sheet) with a solid-purple-blue line. Indeed, C2 crosses first the current since the intersatellite distance between C2 and C3 (along the Z-axis) is ΔZ=1780 km; C2 is closer to the neutral sheet than C3. Around t_1, the C2-B_y is negative, whereas the C3-B_y positive. Exactly the same occurs around t_2. At t_3, only C2 is appropriately located to detect a significant negative B_y excursion. In between t_1 and t_2 the C3-B_y excursion has to be negative, as it is actually the situation. Around each of the three major C2-B_y excursions, the bipolar B_z signature is readily readable; obviously the case of Ew plasma flow matches with the Tr-1 trajectory in Fig. 1. Consequently, the suggested sketch of Fig. 7 gives a satisfactory reproduction for the main magnetic field perturbations.

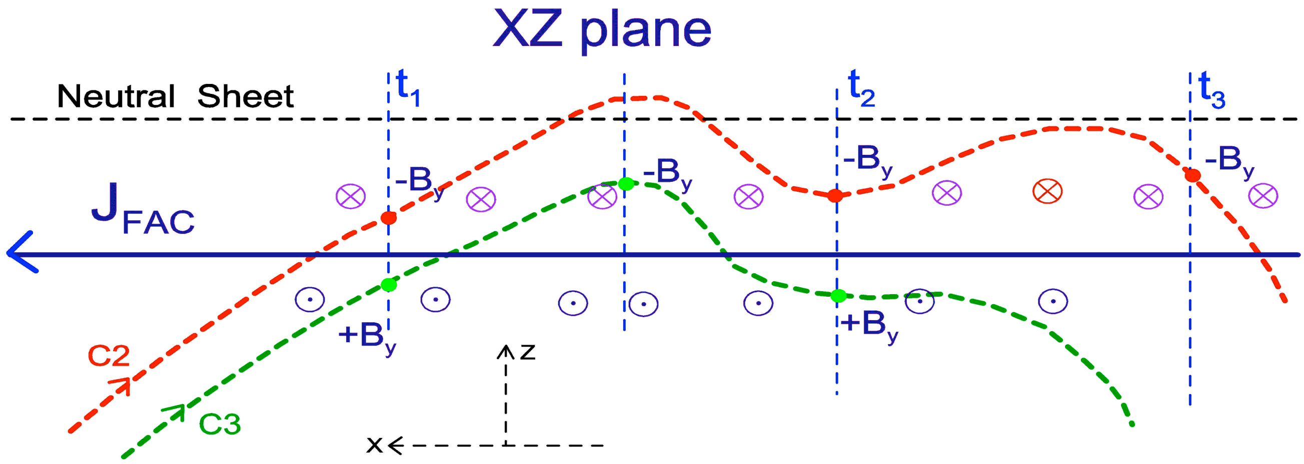

Fig. 7. C2 (red path) and C3 (green path) are sketched moving (over the XZ plane) from the south lobe to neutral sheet and then back to their points of departure; thus they are engaged with the one branch from the dual filamentary system of FACs. At the successive time moments t_1, t_2 and t_3 (corresponding to those set in Fig. 6), three major negative B_y deflections are detected by C2. In particular, at times t_1 and t_2, opposite polarities for the B_y deflections are detected by C3 and C2.

3.4. Third Event, a Double MFR-Like Structure

Figure 8 (with the same format as Fig. 5) clearly shows two successive MFR-like structures occurred with tailward (Tw) plasma flow and captured by C2 (thin-red line) and C4 (thick-blue line). The positive excursions of B_y (occurred at t_1 and t_3) along with the associated bipolar signatures of B_z are apparent for both potential rope structures. Certainly, the total magnetic field increases are not as profound as in the preceded events; the spacecraft stay very close or go toward the lobe. Nevertheless, they probably exist. At time t_2 (in between t_1 and t_3, marked by the vertical dashed-blue line) the B_y reaches negative values at C4. It is especially meaningful to focus on the interval around time t_3 wherein the peak values of B_y for different Cluster satellites are clearly time-shifted. Indeed, all the four satellites recorded different arrival times for the B_y excursion, as it is evident in **Fig. 9** (third panel). First, it is detected by C2; then as the C2-B_y declines the disturbance is recorded by C4. And progressively, it is detected by C3 and even later by C1, though much weaker. The measured delay times between C2C4, C4C3 and C3C1 are 1.8, 2.5 and 3.1 s, respectively. What is the ultimate cause for the well-ordered B_y perturbation?

Interpretation: If we take a look at the spacecraft placement over the XY plane (**Fig. 10a**), then we shall probably be convinced about their origin. It seems that the B_y disturbance front clearly propagates dawnward with an estimated velocity of V_y=270 kms^{-1}, and the front is slightly inclined relatively to the X-axis. The B_y excursion is short-lived with duration ~5 s. It is worth noticing that, if the B_y structure was really the core of a rope, then the diametrically opposite should be observed: for a "B_y core", largely extended along the Y-axis, no delays would be anticipated (given that Cluster is moving dawnward). And we have to point out that the B_y excursions occur adjacent to the north lobe plasma sheet. later on, all the four satellites move toward the CPS and eventually cross the neutral sheet. **We infer that in this situation there is strong evidence for an earthward flowing filamentary current that propagates dawnward, too.** The situation seems to be crystal clear; when the filamentary current successively passes overhead the C2, C4 and C3 satellites (as it is visualized by the J_{FAC} arrows in Fig. 10a), the B_y is peaked. In conclusion, **the filamentary current seems to flow within a channel with thickness less than 1000 km.** As far as C1 is considered, it seems that the filamentary current stands away from it; accordingly, the C1-B_y is slightly affected.

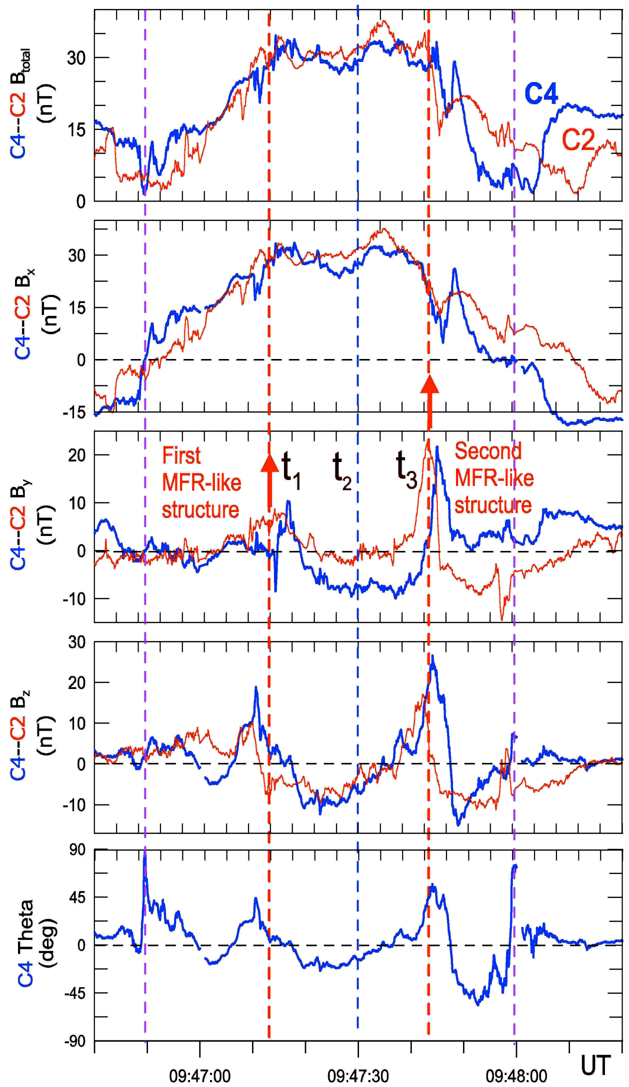

Fig. 8. An 100-s interval showing the magnetic field signatures corresponding to two distinct MFR-like structures observed by C2 (red-thin line) and C4 (blue-thick line) with tailward plasma flows. At the bottom panel the theta-polar angle of the magnetic field is shown for C4.

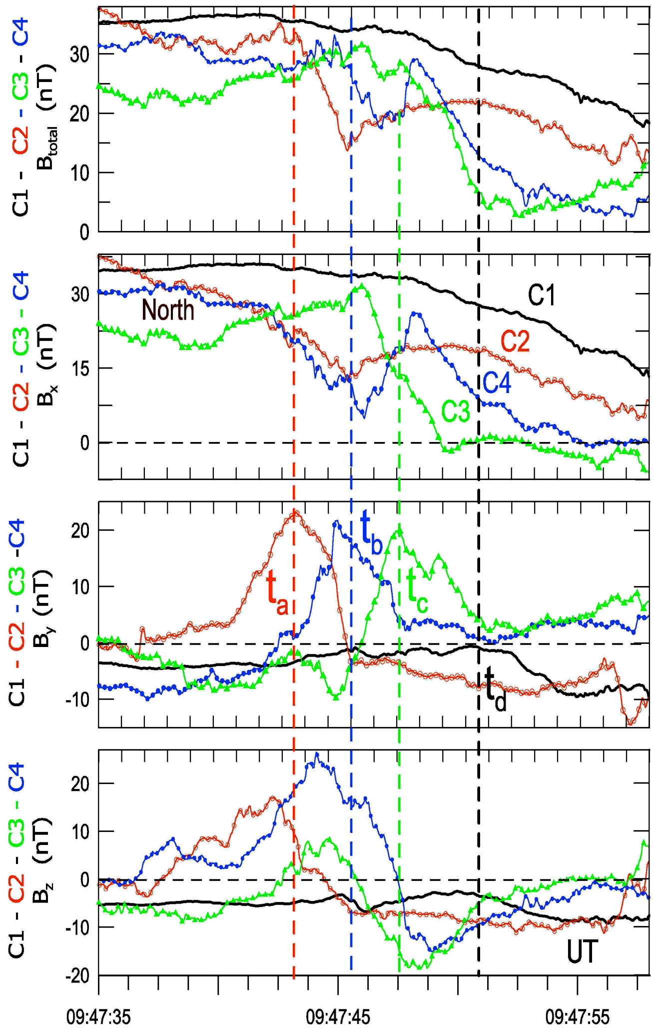

Fig. 9. Vector magnetic field datasets for all the Cluster satellites concerning the second MFR-like structure of Fig. 8. The systematic time-shifted B_y deflections (third panel) are probably produced by a dawnward propagating filamentary current (shown in Fig. 10); the current flows earthward along the magnetic field lines.

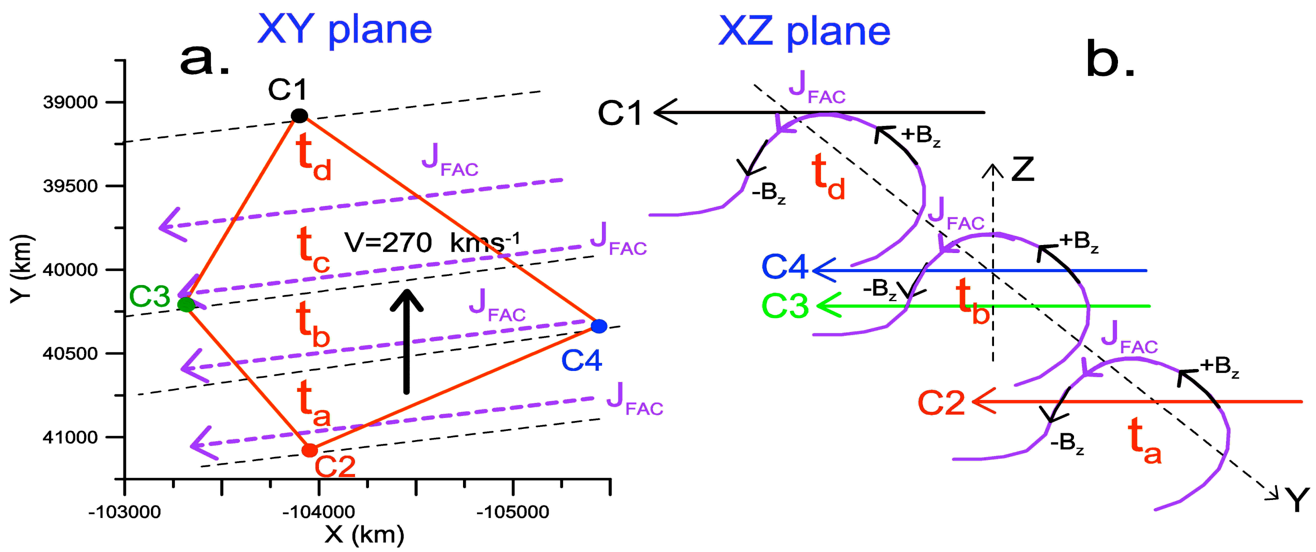

Fig. 10. (a) A dawnward propagating filamentary current (thick-dashed arrows over the XY plane) is successively passing through the Cluster tetrahedron. The current is flowing earthward along the magnetic field lines, while the Cluster tetrahedron is projected over the XY plane. The current velocity V_y is about -270 km s^{-1}. (b) The satellites traversing the "ion capsule region" are shown over the XZ plane, at different times.

Besides the dawnward motion of filamentary current (over the XY plane), we have to assume one more motion imposed by the Tw plasma flow: Cluster has to run along a trajectory like the Tr-2 in Fig. 1. The bipolar $+B_z/-B_z$ signatures are clear for C2, C3 (not shown) and C4 (Fig. 8). The C2 signature is preceded those of C3 and C4; a result that can be derived from the appropriate satellite crossing of the 3-D MFR-like structure over the XZ plane. As one can see in **Fig. 10b**, C3 and C4 simultaneously encounter the $+B_z/-B_z$ signature around t_b. Obviously, the dawnward propagation delay (from C4 to C3) compensates the tailward propagation delay (from C3 to C4). Moreover, the C1-B_y excursion is negative since the C1-B_x value is more than 15 nT larger than those of C2-B_x and C3-B_x; consequently, the current flows mostly below C1, as it is shown in Fig. 10b.

The "first MFR-like" signatures (Fig. 8) may be produced in a similar way, but the much weaker current (in this situation) is not sufficiently filamentary, too. In general, it seems that the associated FAC intensity is variable in time and space. However, there are similarities with the "second MFR": (a) the C1-ΔB_y deflection is also weak (not shown here), whereas the ΔB_y deflections at C2, C3 and C4 are much stronger, and (b) the current flows adjacent to the plasma sheet/lobe interface, too.

Finally, it is worth noticing that throughout the event the sketched FAC shows the appropriate polar angle variations in accordance with those dictated by the B_z traces. Actually, we discern the two successive bipolar (north-then-south) signatures of B_z at t_1 and t_3. In addition, it is rather constructive to look at the polar-theta angle trace of, for instance, C4 (Fig. 8, bottom panel). At the times of "ropes" this angle reaches the value of ~50^o, a fact that supports our current waveform adopted in Fig. 1. It is noticeable that the two neutral sheet crossings of C4 (marked with vertical-dashed lines, too) are accompanied by very large theta angles; the plasma sheet close to the neutral sheet indeed demonstrates the normal geometry. In conclusion: The introduced filamentary FAC self-consistently explains all the major observed signatures of the Cluster magnetic field.

3.5. Supplementary Observations

After the already presented intervals, one may conjecture that throughout the whole studied interval (of 9 min, Fig. 3) all the remaining major magnetic field features may be well produced from the same dual system of earthward flowing filamentary currents, too. Are there FACs unceasingly at work? A positive answer wouldn't sound like an arbitrary generalization or exaggeration; in contrast, it seems to be a verifiable fact. To this direction, it is meaningful to briefly scrutinize the non-presented subintervals. In these (four) subintervals, although we do not identify distinct MFR-like structures, however, significant B_y excursions of opposite polarities are systematically observed by satellites positioned within the plasma sheet at almost symmetrical sites with respect to the neutral sheet. In the fourth case successive bipolar signatures are currying an particularly important information. Accordingly, we present all the four subintervals in Figs 11-14. At the bottom panel of Figs. 11, 12 and 13, the C1 and C3 trajectories are visualized relatively to the suggested system of FACs, over the XZ plane.

First subinterval. In **Fig. 11**, C1 traverses the whole plasma sheet (on the basis of the B_x trace there is a transition from about -27 to 27 nT, second panel), while C3 gradually moves to the neutral sheet. Around t_2, two intense and oppositely directed B_y excursions are detected by C1 and C3, while the satellites are positioned somewhere between lobes and CPS. A result that easily can be produced by two filamentary FACs situated close to the lobes (schematic at the bottom). Black-dashed and -green lines correspond to the C1 and C3 tracks, respectively. Additionally, C1 at t_1 observes B_y excursion with opposite sign as compared to that at t_2; at t_1 and t_2, C1 seems to be equally distanced from neutral sheet.

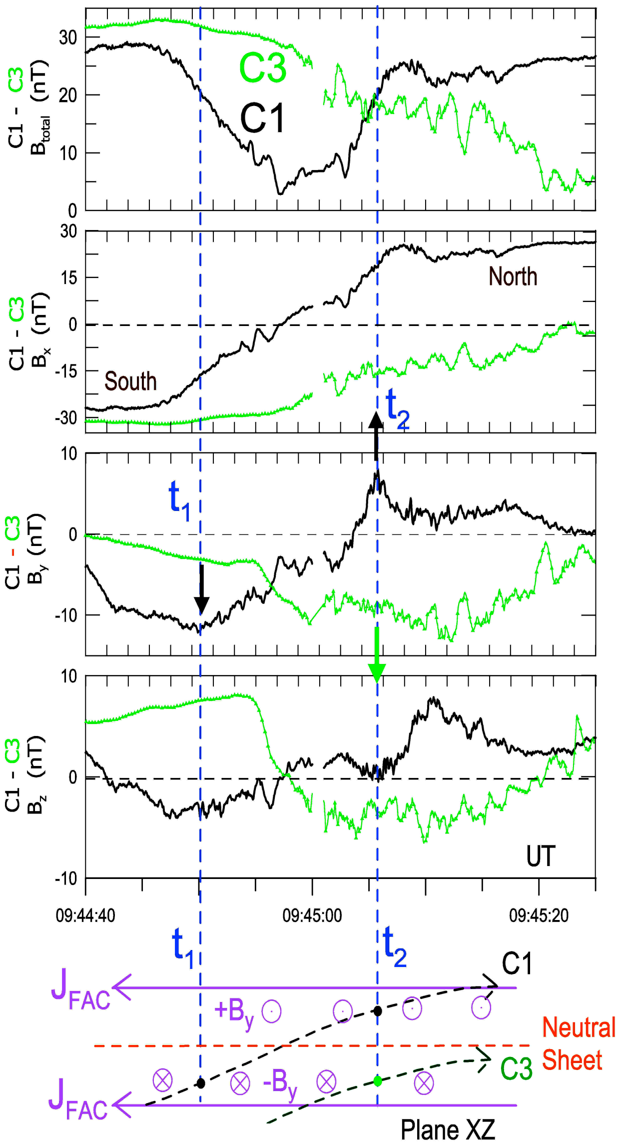

Fig. 11. Magnetic field datasets demonstrating that C1 and C3 positioned in northern and southern plasma sheet, respectively, detect oppositely directed By deflections (at time t_2). The B_x trace provides the spatial information used in the insert sketch showing the spacecraft trajectories relatively to the system of dual filamentary FACs.

Second subinterval. In **Fig. 12** and for the period confined in between the two vertical-dashed lines, from time t_1 to t_2, C1 and C3 were situated at almost symmetric positions relatively to the neutral sheet. The distinctly different responses seen along the B_y traces (i.e., positive excursion for C1 and negative for C3) are probably an outcome caused by an assumed dual filamentary current system. At the bottom schematic, one can see the satellite tracks related to FACs over the XZ plane. The two current branches flow earthward and close to the lobes. The red-dashed line, in third panel, is the fourth degree polynomial fitting for the highly variable C2-B_y trace; C2 is positioned very close to neutral sheet.

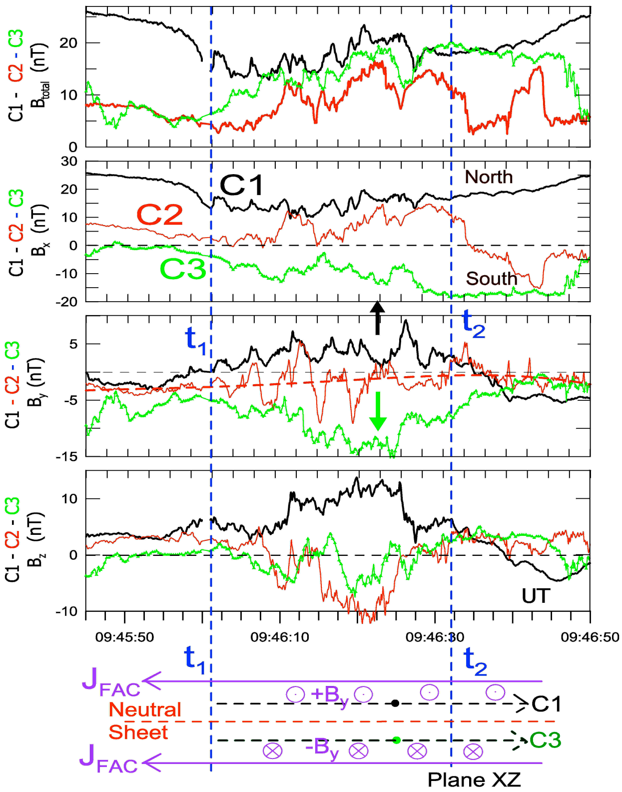

Fig. 12. Much like as for the preceded interval of Fig. 11: in between t_1 and t_2, C1 and C3 positioned in northern and southern plasma sheet, respectively, detect oppositely directed B_y deflections.

Third subinterval. Within the plasma sheet and around t_o (marked by the dashed-vertical line) C1 and C3 move southward (**Fig. 13**, second panel); C1 from the north lobe toward neutral sheet, and C3 from the neutral sheet toward south lobe. At t_o, C1 and C3 record B_y excursions with opposite polarities. The sign of B_y is consistent with the sketched (earthward flowing) filamentary currents at the bottom panel. C2 moving from the northern CPS toward the southern CPS impressively reaffirms the transition from a plasma regime dominated by positive B_y values to a new one dominated by negative B_y values; at t_o, C2-B_y is zero.

Fourth subinterval. First we pay attention at Cluster's exit out of the north plasma sheet, and especially at the four successive $+B_z/-B_z$ bipolar signatures occurring around t_1, t_2, t_3 and t_4 (**Fig. 14**, bottom panel). In this work context, we suppose that an Ew directed FAC, flowing adjacent to the north lobe plasma sheet, passes through the Cluster tetrahedron as it is shown in **Fig. 15**, where the satellites are projected over the XY plane along with the supposed J_{xy} current over the same plane. The current direction (being parallel to the B_{xy} vector) is tilted ~20^o relatively to the X-axis. The $\pm B_z$ magnetic field variations associated with the current will produce the four successive $+B_z/-B_z$ bipolar transitions detected at times t_1-t_4 in Fig. 14. The current velocity is estimated ~200 kms^{-1}. It is worth noticing that the Cluster exit out of the north plasma sheet is not caused by its vertical (along the Z-axis) displacement; essentially, the Cluster is moving dawnward, or more accurately, the entire tilted magnetotail is moving duskward. The case is already clearly sketched in Fig. 2; thus, it is reasonable that the B_y trace do not display any significant bipolar variation. Under the same scenario a similar FAC is anticipated flowing Ew somewhere close to the south lobe and plasma sheet interface. Actually, C3 and C4, at their entries into the plasma sheet, detect $+B_z/-B_z$ bipolar signatures, too. Hence, along a complete plasma sheet crossing, C3 and C4 display twice the same $+B_z/-B_z$ bipolar signature.

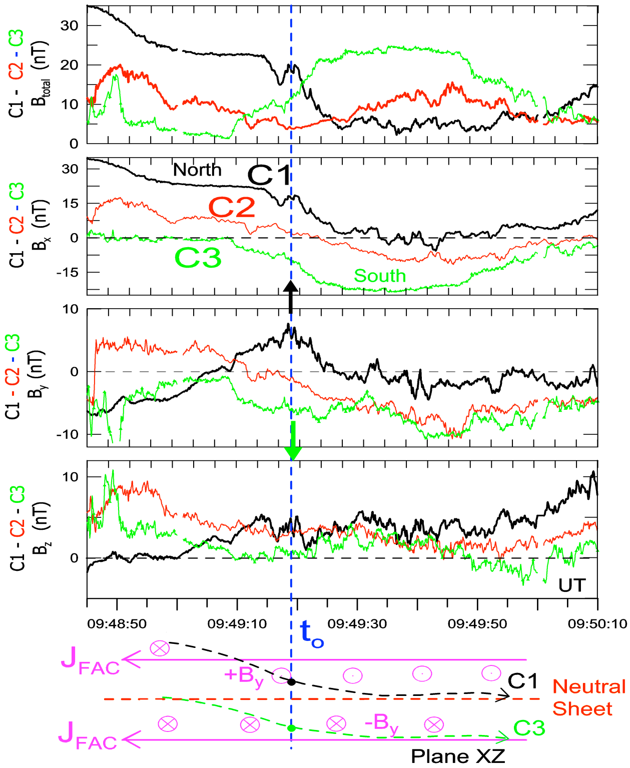

Fig. 13. Much like as for the preceded interval of Fig. 11: at t_o, C1 and C3 positioned in northern and southern plasma sheet, respectively, detect oppositely directed B_y deflections.

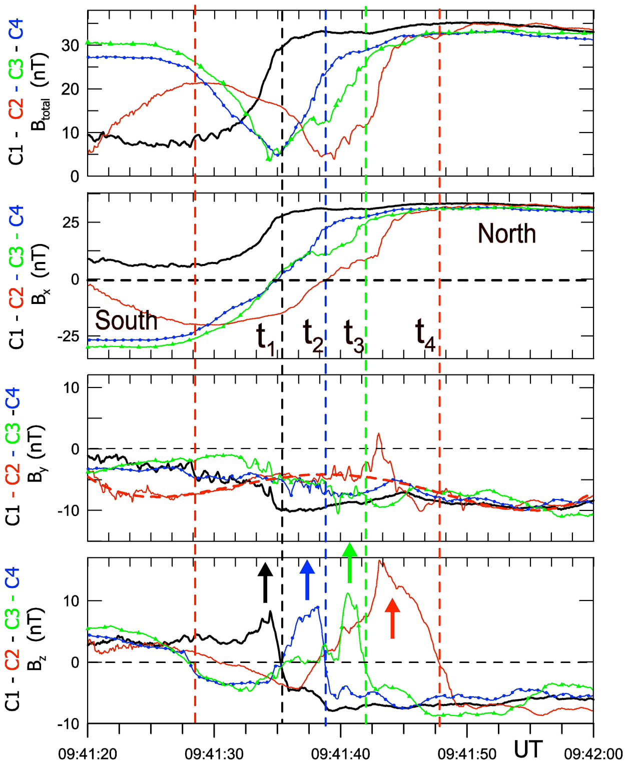

Fig. 14. During the tail's crossing from south to north lobe C3 and C4 display twice the same $+B_z/-B_z$ bipolar signature, a situation corresponding to the satellite trajectory of Fig. 2.

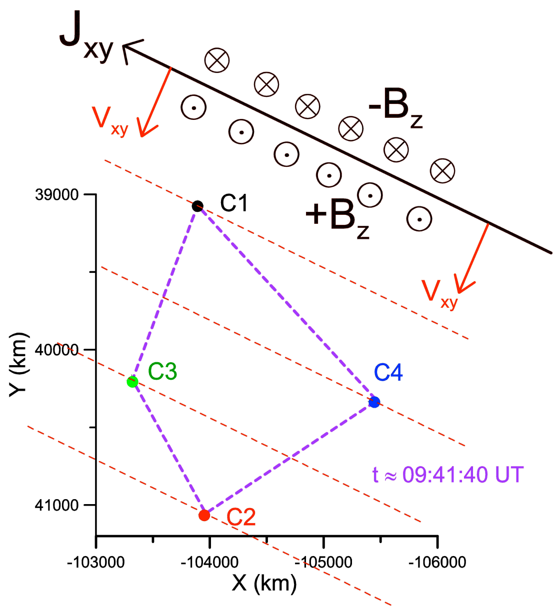

Fig. 15. An almost earthward directed FAC, flowing adjacent to the north lobe plasma sheet boundary, passes through the Cluster tetrahedron. The spacecraft projections over the XY plane are shown along with the supposed J_{xy} current being parallel to the $\boldsymbol{B}_{xy}$ vector. The current is tilted ~20° relatively to the X-axis. The $\pm B_z$ magnetic field variations associated with the current will produce four successive $+B_z/-B_z$ bipolar transitions, as they are seen at times t_1, t_2, t_3 and t_4 in Fig. 14. The current velocity is estimated ~200 kms^{-1}.

4. Discussion

4.1. B_y Deviations Not Dictated By IMF

In the Earth's magnetotail, the magnetic field B_y is generally attributed to IMF driving and smaller-scale internal dynamics. Petrukovich [13, 14] constructed a new detailed statistical model of plasma sheet B_y and targeted his investigation on the origins of quasi stationary plasma sheet B_y. They used 15-min Geotail averaged data and inferred that the IMF B_y penetration for the whole data set was 0.35. However, although B_y is mainly driven by IMF, they concluded that there is a contribution of dipole tilt that depends on the magnetosphere flank and season. This dipole tilt effect is maximal in the pre-midnight sector, where several tilt contributions sum up, and can be comparable with the IMF driving. In our case the dipole tilt angle effect would be of great importance on the basis of Cluster location, but the dipole tilt angle is small, -5.7°, and therefore its contribution to the B_y budget is little. In addition, it should be stressed that we study B_y variations lasting less than 15 s; for instance we observe two oppositely directed B_y deviations separated by only 10 s (Fig. 5). Apparently, within 9 min, our observed B_y deflections show distinct, positive and negative values. Thus investigations based on 15-min averages are essentially inappropriate to account for the presented B_y signatures. **The internal magnetosphere dynamics seems to surpass any influence caused by the IMF B_y penetration** or the dipole tilt angle.

The Cluster tetrahedron was situated in the Earth's magnetotail, at X= -16.3 R_E, while at the same time Geotail was located upstream of the bow shock, at X=17 R_E. The solar wind velocity was V_x= -480 Kms^{-1} and the resulting propagation time is ~6 min. Therefore, Geotail provides the unique opportunity to undoubtedly determine any existing relationship between the IMF-B_y and MFR-B_y polarities for each case, one by one. The vector magnetic field measurements of Geotail are given in **Fig. 16**, in the GSM coordinate system; the three vertical-red-dashed lines indicate the occurrence times corresponding to the three studied events. As we shall infer below the B_y deviations, for the majority of MFR-like structures, is doubtlessly not dictated by the IMF-B_y:

At ~09:43 UT, C2 recorded B_y= -23 nT (Fig. 3), whereas the corresponding IMF-B_y = 6 nT (Fig. 16, first vertical-dashed line).

Around 09:44 UT, C2 recorded three peaked B_y values with the major being -34 nT (Fig. 4), whereas the IMF-B_y= 5.5 nT (Fig. 16, second vertical-red-dashed line).

Around 09:47:30 UT, C2 recorded two positive deflections of B_y with the major being 23 nT (Fig. 5); they corresponds to IMF-B_y = 6 nT (Fig. 16).

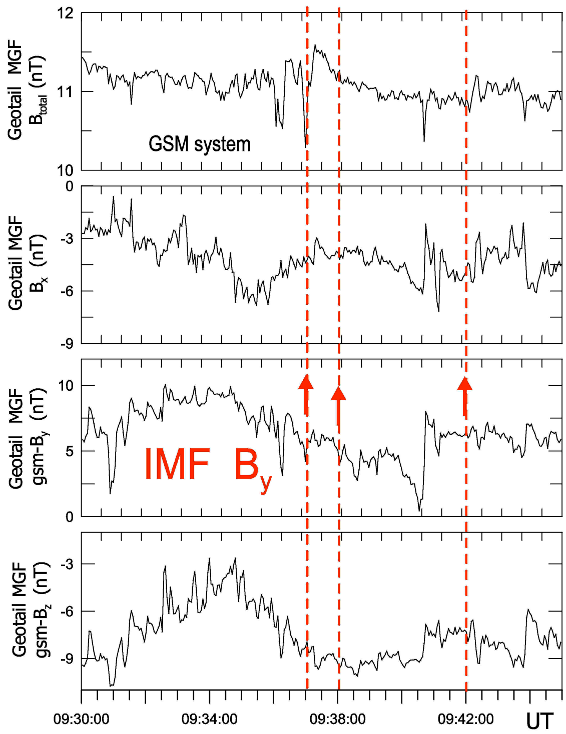

Fig.16. Vector magnetic field measurements for the IMF recorded by Geotail upstream of the bow shock. The three vertical red-dashed lines correspond to the main events marked in Fig. 3 with thick-dashed-red vertical lines. The B_y throughout the whole interval is steadily positive, although we detect MFR-like structures with strong negative B_y excursions. The propagation time between Geotail and Cluster is ~6 min. Only theses data are shown in the GSM coordinate system.

Therefore, in four out of seven "MFR-like episodes", the B_y has exactly the opposite polarity than that of the IMF-B_y. Finally, the observed strong B_y deflections are entirely unrelated to any IMF-B_y polarity. This profound antithesis from what one would anticipate [9-12], in terms of the magnetic field reconnection model, must lead us to a different production mechanism for the B_y deflections. Our events do not line up to the classical view of reconnection presumably producing the rope's core in the Earth's magnetotail under the influence of the IMF; **a concept apparently not at work.** The latter undoubtedly leads us to the conclusion that the studied structures are probably related to filamentary field-aligned currents. At times, the wavy modulated filamentary FACs may be recognized as a rope; actually it is a so-called pseudo-MFR. It is already stressed that the duration of the presently studied structures is ~10 s, whereas the duration for a typical MFR is ~ 100 s, a difference of an order of magnitude. We also note that, in the GSE coordinate system, the IMF-B_y values are more positive than those shown in Fig. 16.

4.2. More Disagreements with "Genuine MFRs"

The MFR in literature is treated as an entity composed of the helical outer layer of magnetic field and the inner core along its main axis; the core's axis in magnetotail is essentially perpendicular to the XZ plane and presumably lies on the neutral sheet plane. Based on this model and adopting the possibility of multiple reconnection sites, we can draw a representative sketch, which is frequently given in the past and recent bibliography (e.g., [37, 38]). A similar drawing, with three successive MFRs over the XZ and XY planes, is shown in **Fig. 17**. Certainly these closed structures display, in general, similar B_y and B_z signatures with those studied in this work; however, the presented MFR-like structures seriously deviate from this picture. For instance, throughout the studied 9-min interval in this work, **one can identify six cases in which strong positive and negative B_y deflections are simultaneously observed by different satellites.** These cases are already discussed and are clearly shown in Figs. 5 (between C2 and C3, at t_2), 6 (between C2 and C3, at t_1, and t_2) 11, 12 and 13 (between C1 and C3). In other cases we observe that the B_y deflections change sign alternately (e.g., C3-B_y in Figs. 5), thus arriving at a plausibly question how these cycles could be produced by multiple reconnection centers. An additional worth noticing point is that satellites positioned farther off the neutral sheet frequently measure higher B_y values (e.g., Figs. 5, 8, 11 and 13 at t_o).

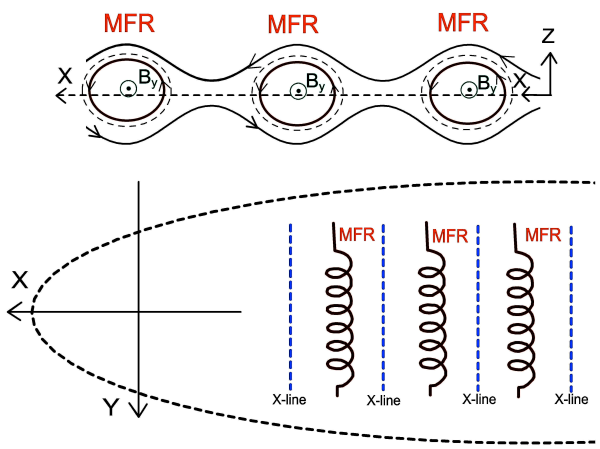

Fig. 17. Schematic illustrating three successive MFRs, in the Earth's magnetotail, formed as a result of multiple reconnection neutral lines in the XZ and XY planes. Each MFR is assumed as a spatial structure moving earthward or tailward. The helical structure of the magnetic field as well as the B_y core for each rope is apparently visible.

4.3. Reconnection's Hall Currents and the Polarity of B_y Excursions

Collisionless reconnection in the Earth's magnetotail is considered as one of the most important and most fundamental energy release processes in collisionless plasmas. In this process, Sonnerup [39] was the first to realize the importance of Hall currents resulting by the different behaviour of electrons and ions within the ion diffusion region. The Hall currents are defined as flowing strictly transverse to the electric and magnetic fields. The magnetized electrons, in the outflow plasma region, are moving outward with velocity $u_x=E_y/B_z$, where E_y is the cross-tail convection electric field. The electron Hall currents are $j_H = -enE_y/B_z$ and (in the ion inertial region) generate a weak out-of-plane quadrupolar field which plays the role of a weak guide field, as it is shown in **Fig. 18** (outflow regions, blue symbols). Therefore, the Hall currents are an indication of two facts: The collisionless nature of the plasma inside the ion inertial domain (possibly with the exclusion of the electron inertial region) and the presence of reconnection in the current layer. Thus, it may be interesting to scrutinize all our cases characterized by very intense B_y deviations: we inspect whether the observed B_y deflections actually comply with the above theoretical picture of reconnection and the associated Hall currents.

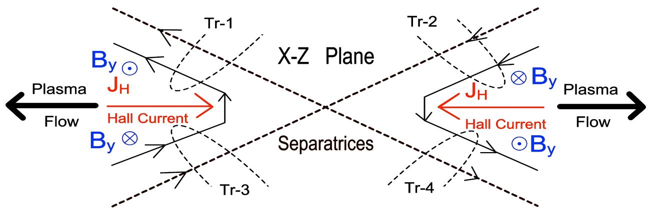

Fig. 18. Schema of two-dimensional Hall current system over the XZ plane (associated with collisionless reconnection in thin current sheets) for the outflow regions along with the B_y magnetic field excursions. The Hall current is flowing antiparallel to the outward convecting electrons and perpendicular to both the convection electric field and the B_z component of the magnetic field. Indicative satellite trajectories are shown in dashed-black lines.

First case study (Fig. 5): Indeed the major excursions of C2-B_y and C3- B_y in north plasma sheet are positive, and in south plasma sheet are negative, given that the plasma flows earthward; a result that **entirely lines up with the Hall current model**. The associated trajectories as shown in Fig. 18 are Tr-1 and Tr-3. Certainly, in this context one has to answer the question how the B_y excursions (produced by Hall currents) are simultaneously related to the B_z bipolar signatures.

Second case study (Fig. 6): C2 (positioned close to the neutral sheet) measures three successive negative B_y excursions at the south hemisphere of plasma sheet with earthward plasma flows. The situation corresponds to the trajectory Tr-3 of Fig. 18; it seems that there is not any contradiction with the Hall current. Again, one has to explain (in the Hall current context) how the B_z trace is associated with three successive bipolar signatures (corresponding to the three MFR-like structures).

Third case study (Fig. 8): C2 and C4 located in the north plasma sheet record tailward plasma flows; the case corresponds to the trajectory Tr-2 of Fig. 18. The observation of two positive B_y deflections seems to conflict with the theoretical model of Hall currents (according to which negative B_y excursions are anticipated); moreover, the major B_y deviation is so strong as 20 nT. In this situation we have introduced an earthward flowing filamentary current (adjacent to the north lobe plasma sheet) that suffices to produce the observed magnetic field signatures.

However, one may argue that there is not actually the

Hall current that produces the B_y excursions (in the third case study), but the excursions are produced by FACs diverging from the Hall current. In that case we need a tailward flowing FAC close to the north lobe. Thus, we shall discuss this case in more detail. We have to take into account three significant elements: (a) Cluster is very close to the supposed X-line, since the plasma flow is just switched from earthward to tailward, (b) the plasma sheet is constantly very thin: actually, for the first event its thickness is estimated ~1750 km; C2 and C3 cross the plasma sheet within 25 s. In the second event, C1 (C4) at t_1 is located close to north (south) lobe (not shown); thus the plasma sheet thickness is ~1000 km, and C1 crosses the plasma sheet within 25 s. Similarly, in the third event, C4 crosses the north plasma sheet within 20 s, and (c) the positive excursion of C2-B_y in Fig. 5 seems to occur at the same site in plasma sheet with the positive excursion of C2-B_y in Fig. 8, at the moment t_3; however in between them there is opposite direction of plasma flow. Thus, if the case of Fig. 5 is accepted that entirely complies with the Hall current system, then one is forced to infer that **the case of Fig. 8 completely fails to line up with the Hall current hypothesis**. In any case, we have to observe similar cases (with tailward plasma flows) in the future, for a more reliable conclusion.

4.4. The Filamentary Currents Associated with the First and Third Events

The "second MFR-like" episode presented in Fig. 8 is an excellent example demonstrating that the supposed B_y core is nothing more than **a spatially limited disturbance**; the B_y is not actually a core extended across the tail. In addition, B_y propagates dawnward with velocity V_y=270 kms^{-1}, and the estimated ΔY-thickness for the filamentary current (being the ultimate B_y source) is less than 1000 km. Thus, we infer that each satellite is affected ~5 s by the FAC; **the life of B_y is depended on the propagation velocity of the filamentary current**. The Cluster tetrahedron plays a decisive role in discriminating between temporal and spatial effects; it reveals that the hypothetic B_y deviation is nothing more than a short-lived ephemeral perturbation. Finally, the studied MFR-like structure does not seem to be a long-lived helical structure of magnetic field embedded in plasma flow as we used to think about, but **it is a magnetic field perturbation induced by a moving filamentary current according to Ampere's law**.

In the first case study, we simultaneously observe (Fig. 5, at t_2) positive and negative B_y excursions for C2 and C3, roughly located in mid-north and mid-south plasma sheet, respectively. In our interpretation scheme, we have introduced two branches of filamentary FACs, which are symmetrically placed with respect to neutral sheet, as the appropriate ultimate sources for the strong B_y excursions.

One has to pay particular attention to these episodes in order to really discriminate between **FAC effects or rope configurations**. Based on our results, if one is analyzing single satellite measurements characterized by the morphological magnetic field signatures usually encountered in MFRs, then probably he studies "pseudo-MFRs".

4.5. A Few More Comments

Obviously a very prominent result (in this work) is that tens of B_y and B_z signatures, observed during an interval of no more than 9 min, can be well produced by two branches of filamentary FACs. Our suggestion concerning the specific mechanism producing these FACs is based on a recent work by Sarafopoulos [1] introducing a twin-double layer (DL) structure as the ultimate source having the capability to launch high velocity ion jets on opposite directions along the tail; the proposed model is exhibited in subsection 2. Therefore, the observational part of this work is well associated with the interpretative one, as already stated in the Introduction to this work. An emphasis that inheres in this work is that the pseudo-MFRs are rather commonly occurring in the Earth's magnetotail, they are the effects of filamentary FACs. Snekvik et al., [40] well reproduced the signatures from one MFR-like structure based on FACs; the research concerning the mechanism supplying these currents must be of high priority in the future.

Frequently in mainstream research may be an indiscriminate usage of Fig. 17 composed of successive closed magnetic structures. In the context of this work, the proposed loop-like topology may mimic certain of our observations, but eventually fails to give an overall self-consistent explanation.

We propose the filamentary FAC waveforms as a working hypothesis. If this model is further established in the future, then we can estimate the current densities using the curlometer technique [41]. The results of this technique are largely depended on the interpretation model. The CLUSTER tetrahedron is extended along the Z-axis slightly less than the plasma sheet thickness or the distance between the two parallel currents (for instance look at the "first event"). Thus, as the CLUSTER approaches the northern branch of FAC or recede from the southern branch of FAC, the J_x (i.e., the curlB_y) has to be positive. In between the two filamentary currents the J_y (i.e., the curlB_x) has to be maximized as due to the current sheet, while the curlB_y will probably give a negative value for the J_x. The latter is actually the case for the "first event" (not shown here); and the negative J_x is obviously an artifact due to the technique; such a current probably does not exist at all. The two earthward flowing filamentary currents just outside the tetrahedron are seen (using the technique) as a tailward flowing current threading the tetrahedron. Thus, we first have to choose the interpretation model and then apply the technique.

5. Conclusions

We study a 9-min interval in which a large amount of bipolar and monopolar B_y and B_z deviations, irrespectively of being parts or not of MFR-like structures, could be well produced by a dual system of FACs persistently flowing earthward; one branch in northern and the other in southern plasma sheet; thus, the B_y deviations seem to be the effect of Ampere's law throughout the whole studied interval. Most importantly, we simultaneously observe six intense B_y deviations with opposite polarities at different satellites. Additionally, we have shown that the B_y deviations for several MFR-like structures is doubtlessly not dictated by the IMF. The classical view of reconnection directly producing the "B_y core" in plasma sheet under the catalytic influence of the IMF is not working at all in our cases.

Particularly in a case study, it is clear that the MFR-like structure is not "a long-lived magnetic field entity" embedded in plasma flow, as we used to think about "real ropes", but it is actually a local magnetic field perturbation induced by an earthward flowing filamentary current confined (across the tail) in a channel with thickness ΔY less than 1000 km. Finally, we conclude that all the studied structures (in this work) are really pseudo-MFRs; since a non-genuine MFR structure (i.e., an entity composed of a core plus the wrapped-helical magnetic field) has been detected. Amid very high geomagnetic activity, we did not detect any authentic MFR entity that would be probably associated with the dramatic magnetic field reconfigurations inherent in the sketch of Fig. 17. Therefore, special care is required in similar studies discriminating between genuine- and pseudo-MFRs.

The studied B_y deviations are so intense as those in typical MFRs [37, 2]; however, their duration is ~10 s, whereas in typical ropes the duration is ~100 s. If actually the core of a typical rope is produced by an ion vortex (i.e., a circular ion current formed in magnetotail under specific conditions, as it is recently suggested by Sarafopoulos, [2]), then we can infer that the presented MFR-like structures are not directly related to the circular ion current; rather they are related to the FACs. This work stresses the role of FACs interconnecting the ionosphere with the "ion vortex" in tail, while the work of Sarafopoulos [2] emphasizes on the mechanism via which the rope's core is originated by a cyclic ion current. In the former case the B_y deviations may last for a few seconds up to tens of minutes [2], while in the latter case they last for 1-2 min. In both approaches our main purpose is to identify the rope's current system.

We interpret earthward flowing (filamentary) FACs as the result of intense ion jets produced by a twin-DL system; the latter is introduced by Sarafopoulos [1] and plays a role similar to that of an X-type reconnection line launching plasma jets. The always earthward flowing FACs are neutralizing the positive charges and it seems to be a profound feature; the magnetic reconnection theory does not completely comply with this aspect of dynamics. Needless to say that, specifically in our situation with persistently flowing FACs, the current (and not the magnetic field) is the fundamental quantity. The twin-DL entity dissipates magnetic field energy stored in the tail; it is associating, in a natural way, the local and global magneto-plasma processes in the Earth's magnetotail.

6. Acknowledgements.

We thank the Principal Investigators (a) E. Lucek, of the Cluster FGM (Fluxgate Magnetometer) datasets, (b) Henri Rème, of the Cluster CIS (Cluster Ion Spectrometry) experiment, and (c) S. Kokubun for the high-resolution Geotail/MGF magnetic field data. This research has been co-financed by the European Union (European Social Fund- ESF) and Greek national funds through the Operational Program "Education and Lifelong Learning" of the National Strategic Reference Framework (NSRF)-Research Funding Program: Thales. Investing in knowledge society through the European Social Fund. The project is called "Hellenic National Network for Space Weather Research" coded as MIS 377274.

European Union European Social Fund
OPERATIONAL PROGRAMME EDUCATION AND LIFELONG LEARNING investing in knowledge society
MINISTRY OF EDUCATION, LIFELONG LEARNING AND RELIGIOUS AFFAIRS
MANAGING AUTHORITY
NSRF 2007-2013 programme for development
EUROPEAN SOCIAL FUND
Co- financed by Greece and the European Union

References

1. Sarafopoulos, D. V.: Twin-Double Layer Structure Producing Tailward Ion Jets in the Earth's Magnetosphere, Journal of Engineering Science and Technology Review, 5(2), 76-84, 2012.
2. Sarafopoulos, D. V.: What does determine the sign of core in Magnetic Flux Rope structures of the Earth's magnetotail, is submitted for publication, 2013.
3. Sarafopoulos, D. V.: A pseudo-magnetic flux rope observed by the THEMIS satellites in the Earth's magnetotail, Journal of Atmospheric and Solar-Terrestrial Physics, 73, 2279-2288, 2011.
4. Lui, A. T. Y., Dunlop, M. W., Rème, H., Kistler, L. M., Gustafsson, G., and Zong, Q.-G.: Internal structure of a magnetic flux rope from Cluster observations, Geophys. Res. Lett., 34, L07102, doi:10.1029/2007GL029263, 2007.
5. Schindler, K.: A theory of the substorm mechanism, J. Geophys. Res., 79, 2803–2810, 1974.
6. Hones, E. W., Jr.: Substorm processes in the magnetotail: Comments on ''On hot tenuous plasma, fireballs, and boundary layers in the Earth's magnetotail'' by Frank, L. A., Ackerson, K. L., and Lepping, R. P., J. Geophys. Res., 82(35), 5633-5640, 1977.
7. Sibeck, D. G., Siscoe, G. L., Slavin, J. A., Smith, E. J., Bame, S. J., and Scarf F. L.: Magnetotail flux ropes, Geophys. Res. Lett., 11(10), 1090-1093, 1984.
8. Russell, C. T., and Elphic, R. C.: Initial ISEE magnetometer results: Magnetopause observations, Space Sci. Rev., 22, 681–715, 1978.
9. Cowley, S. W. H.: Magnetospheric asymmetries associated with the Y-component of the IMF, Planet. Space Sci., 29, 79–96, 1981.
10. Hughes, W. J., and Sibeck, D. G.: On the three dimensional structure of plasmoids, Geophys. Res. Lett., 14(6), 636-639, 1987.
11. Birn, J., Hesse, M., and Schindler, K.: Filamentary structure of a three dimensional plasmoid, J. Geophys. Res., 94(A1), 241-251, 1989.
12. Moldwin, M. B., and Hughes, W. J.: Plasmoids as Magnetic flux ropes, J. Geophys. Res., 96, 14,051-14064, 1991.
13. Petrukovich, A. A., Dipole tilt effects in plasma sheet B_y: statistical model and extreme values, Ann. Geophys., 27, 1343–1352, 2009.
14. Petrukovich, A. A., Origins of plasma sheet B_y, J. Geophys. Res., 116, A07217, doi:10.1029/2010JA016386, 2011.
15. Moldwin, M. B., and Hughes, W. J.: On the formation and evolution of plasmoids: A survey of ISEE 3 Geotail data, J. Geophys. Res., 97, 19259-19282, 1992.
16. Moldwin, M. B., and Hughes, W. J.: Observations of earthward and tailward propagating flux rope plasmoids: Expanding the plasmoid model of geomagnetic substorms, J. Geophys. Res., 99, 183-198, 1994.
17. Lepping, R. P., Fairfield, D. H., Jones, J., Frank, L. A., Paterson, W. R., Kokubun, S., and Yamamoto, T.: Cross-tail magnetic flux ropes as observed by the Geotail spacecraft, Geophys. Res. Lett., 22, 1193-1196., 1995.
18. Slavin, J. A., Owen, C. J., Kuznetsova, M. M., and Hesse, M.: ISEE 3 observations of plasmoids with flux rope magnetic topologies, Geophys. Res. Lett., 22(15), 2061-2064, 1995.
19. Ieda, A., Machida, S., Mukai, T., Saito, Y., Yamamoto, T., Nishida, A., Terasawa, T., and Kokubun, S.: Statistical analysis of plasmoid evolution with Geotail observations, J. Geophys. Res., 103(A3), 4453-4465, 1998.

20. Slavin , J. A., Tanskanen, E. I. Hesse, , M., Owen, C. J. , Dunlop, M. W., Imber, S., Lucek, E. A., Balogh, A., and Glassmeier, K.-H.: Cluster observations of traveling compression regions in the near tail, J. Geophys. Res., 110, A06207, doi:10.1029/2004JA010878, 2005.
21. Zong , Q.-G., Fu, S. Y., Baker, D. N., M. L. Goldstein, P. Song, J. A. Slavin, T. A. Fritz, J. B. Cao, O. Amm, H. Frey, A. Korth, P. W. Daly, H. Reme, A. Pedersen, Earthward flowing plasmoid: Structure and its related ionospheric signature, *J. Geophys. Res.*, 112, A07203, doi:10.1029/2006JA012112, 2007.
22. Amm, O., Nakamura, R., Frey, H. U., Ogawa, Y., Kubyshkina, M., Balogh, A., and Rème, H.: Substorm topology in the ionosphere and magnetosphere during a flux rope event in the magnetotail, Annales Geophysicae, 24, 735–750, 2006.
23. Hasegawa, H., Nakamura, R., Fujimoto, M., Sergeev, V. A., Lucek, E. A., Rème, H., and Khotyaintsev Y.: Reconstruction of a bipolar magnetic signature in an earthward jet in the tail: Flux rope or 3D guide-field reconnection, J. Geophys. Res., 112, A11206, doi:10.1029/2007JA012492, 2007.
24. Lee, L. C.: A review of magnetic reconnection: MHD models, in Physics of the Magnetopause, Geophys. Monogr., vol. 90, edited by P. Song, B. U. O. Sonnerup, and M. F. Thomsen, 139–153, AGU, Washington, D. C., 1995.
25. Baker, D. N., Pulkkinen, T. I., Angelopoulos, V., Baumjohann, W., and McPherron, R.L.: Neutral line model of substorms: Past results and present view, J. Geophys. Res., 101, 12,975-13010, 1996.
26. Lyons, L.: Substorms: Fundamental observational features, distinction from other disturbances, and external triggering, J. Geophys. Res., 101(A6), 13011-13025, 1996.
27. Lui, A., Lopez, R., Anderson B., Takahashi K., Zanetti L., McEntire R., Potemra T., Klumpar D., Greene E., and Strangeway R.: Current Disruptions in the Near-Earth Neutral Sheet Region, J. Geophys. Res., 97(A2), 1461-1480, 1992.
28. Lui, A. T. Y.: Current disruption in the Earth's magnetosphere: Observations and models, J. Geophys. Res., 101, 13067-13088, 1996.
29. Runov, A., R. Nakamura, W. Baumjohann, R. A. Treumann, T. L. Zhang, M. Volwerk, Z. Vörös, A. Balogh, K.-H. Glaßmeier, B. Klecker, H. Rème and L. Kistler.: Current sheet structure near magnetic X-line observed by Cluster, Geophys. Res. Lett., DOI: 10.1029/2002GL016730, 2003.
30. Cattell, C., J. Dombeck, J. Wygant, J. F. Drake, M. Swisdak, M. L. Goldstein, W. Keith, A. Fazakerley, M. André, E. Lucek, and A. Balogh.: Cluster observations of electron holes in association with magnetotail reconnection and comparison to simulations, J. Geophys. Res., 110 , A01211, doi:10.1029/2004JA010519, 2005.
31. Wygant, J. R., C. A. Cattell, R. Lysak, et al.: Cluster observations of an intense normal component of the electric field at a thin reconnecting current sheet in the tail and its role in the shock-like acceleration of the ion fluid into the separatrix region, J. Geophys. Res., 110, A09206, doi:10.1029/2004JA010708, 2005.
32. Runov, A., Nakamura, R., Baumjohann, W.: Multi-point study of the magnetotail current sheet, Advances in Space Research 38, 85–92, 2006.
33. Sarafopoulos, D. V.: A physical mechanism producing suprathermal populations and initiating substorms in the Earth's magnetotail, Ann. Geophysicae, 26, 1617-1639, 2008.
34. Sarafopoulos, D. V.: Bi-layer structure of counterstreaming energetic electron fluxes: a diagnostic tool of the acceleration mechanism in the Earth's magnetotail, Ann. Geophysicae, 28, 455–477, 2010.
35. Balogh, A., Carr, C. M. , Acuña, M. H. et al.: The Cluster magnetic field investigation: Overview of in-flight performance and initial results, Ann. Geophys., 19, 1207– 1217, 2001.
36. Rème, H., Aostin, C., Bosqued, J. M., et al.: First multispacecraft ion measurements in and near the Earth's magnetosphere with the identical Cluster ion spectrometry (CIS) experiment. Ann. Geophys. 19, 1303–1354, 2001.
37. Slavin, J. A., Lepping, R. P., Gjerloev, J., Fairfield, D. H., Hesse, M., Owen, C. J., Moldwin, M. B., Nagai, T., Ieda, A., and Mukai, T.: Geotail observations of magnetic flux ropes in the plasma sheet, J. Geophys. Res., 108(A1), 1015, doi:10.1029/2002JA009557, 2003.
38. Imber, S. M., J. A. Slavin, H. U. Auster, and V. Angelopoulos.: A THEMIS survey of flux ropes and travelling compression regions: Location of the near Earth reconnection site during solar minimum, J. Geophys. Res., 116, A02201, doi:10.1029/2010JA016026, 2011.
39. Sonnerup, B. U. O.: Magnetic field reconnection in Solar System Plasma Physics, vol. 3, edited by L. T. Lanzerotti, C. F. Kennel, and E. N. Parker, pp. 45–108, North Holland, New York, 1979.
40. Snekvik, K., Haaland, S., Østgaard, N., Hasegawa, H., Nakamura, R., Takada, T., Juusola, L., Amm, O., Pitout, F., Rème, H., Klecker, B, and E. A. Lucek.: Cluster observations of a field aligned current at the dawn flank of a bursty bulk flow, Ann. Geophys., 25, 1405–1415, 2007.
41. Dunlop, M. W., D. J. Southwood, K.-H. Glassmeier, and F. M. Neubauer.: Analysis of multipoint magnetometer data, *Adv. Space Res., 8*, (9)273, 1988.